DESIGN & ANALYSIS OF A MEMS INTEGRATED AIRFLOW, HUMIDITY, & TEMPERATURE SENSOR FOR VERTICAL FARMING

V. Bhamidipati[1] and Q. Li[1]
[1]Cornell University, Ithaca, NY, USA

ABSTRACT

Modern vertical farming systems require cost-effective, accurate sensing of environmental factors such as airflow, temperature, & humidity. In this paper, we fabricate, analyze, & simulate an integrated MEMS combined airflow, temperature, & humidity sensor for applications in vertical farming. We employ cantilever structures for the airflow and humidity sensors and thin-film RTD for the temperature sensor. Through COMSOL simulation, we achieve an airflow sensor sensitivity of .2 μm / (m/s) and show that theoretical analysis comes within an order of magnitude of the simulated result. We further demonstrate reasonable isolation from temperature and humidity effects. Future work improving our sensor may enable individual plant-level monitoring for large scale vertical farming systems.

INTRODUCTION

Vertical farming is the agricultural practice of growing crops in vertical layers instead of in horizontal rows, which optimizes land usage and increases the crop yield per unit of land used. Different from traditional farms, vertical farms are mostly located indoors and the controlled-environment agriculture (CEA) technology is applied to control the environmental factors to provide the most favorable environment for the crops to grow in, which could result in a shorter growth time and larger harvest yield. Vertical farming relies on sensors to monitor different environmental parameters. "The most vital [environmental parameters] for plant growth [are] water, CO2, light, nutrients, electricity (for ventilation purposes) and heating" [1]. In our project, we aim to develop a sensor to monitor humidity and temperature to effectively regulate the water and heating parameters. Besides temperature and relative humidity (RH), airflow rate is another significant factor we need to take into consideration since "one of the most influential factors affecting growth in IVFS is to maintain a uniform airflow at an optimal air current speed over plants canopy surfaces" [2].

Since we aim to build a sensor that is used specifically for vertical farming to monitor temperature, relative humidity, and airflow rate, the sensing ranges of our sensor for these three parameters should cover the optimal ranges of these parameters for common crops, which are shown in Table 1.

Table 1: Optimal ranges of relative humidity, temperature, and airflow rate for common crops.

Parameter	Optimal Range
Relative Humidity	50-90% [3]
Temperature	15-37° C [4]
Airflow Rate	.3-.5m/s [2]

In this paper, we first develop three sensors to sense three parameters separately and then integrate them together to ensure that our final design could sense three different parameters simultaneously. For the humidity sensor, L.-T. et al. [5] demonstrate a method to cheaply, accurately, and efficiently measure humidity using a freestanding cantilever. We follow the fabrication processes stated in the paper and choose the length of the beam to enable the sensor to sense the optimal range of RH accurately. Also, L.-T. et al. [5] integrate an RTD-type thermal resistor with their humidity sensor to explore the effects temperature has on the humidity sensor and vice versa. We design our own RTD-type thermal resistor and use this as our temperature sensor by analyzing the relationship between its resistance and temperature. For the airflow sensor, Huicong et al. [6] design a piezoelectric microcantilever to measure the airflow rate. We build a model for the sensor they developed and analyze how airflow rate affects the tip displacement of the beam. With the ultimate goal of incorporating all three sensors on the same silicon, we then combine all three sensors. The integrated humidity, temperature, and airflow sensor we aim to design will enable vertical farms to wholly measure and control these conditions.

FABRICATION AND THEORETICAL ANALYSIS

Temperature Sensor

The temperature sensor we choose is an RTD-type thermal resistor. The resistance of the resistor changes linearly with the change in temperature, which allows us to know the temperature by measuring the resistance. For an RTD-type thermal sensor, the resistance as a function of temperature can be calculated using the following equations:

$$R_0 = \rho L/A \quad (1)$$

$$R = R_0[1 + \alpha(T - T_0)] \quad (2)$$

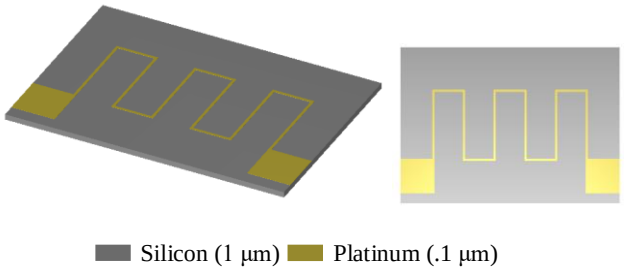

Figure 1: 3D model (left) and top view of RTD-type thermal resistor.

By considering the geometry of our design we arrive at the following equation for the resistance:

$$R_0 = \rho/\{t[NL_v/W_v + (N-1)\rho L_h/W_h]\} \quad (3)$$

Finally, by combining Eq. (2) and Eq.(3), for a N, L_v (length of vertical fingers), W_v (width of vertical fingers), L_h (length of horizontal fingers), W_h (width of horizontal fingers), t (thickness) of 6, 300 μm, 1 μm, 150 μm, 1 μm, and .5 μm, respectively, we find the relationship between the resistance and the temperature:

$$T = 4.71R - 49.814 \quad (4)$$

Humidity Sensor

L.-T. et al. [5] developed three humidity sensor models with different lengths (1500 μm, 3000 μm, and 4450 μm) of the cantilever. Considering the cost of the sensor, we want the length of the beam to be as small as possible while the sensing range of the sensor could cover the range mentioned in Table I, which is

50-90%RH. According to the paper, the upper detection limit for the 1500 μm beam sensor is 70%RH, which makes it unfeasible in our project. Thus, we choose the 3000 μm beam. The model we build in L-Edit is shown in Figure 2.

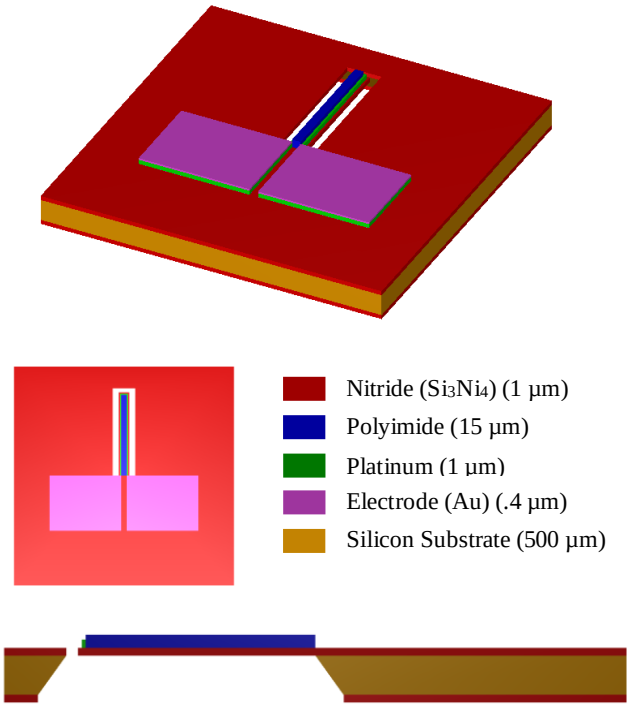

Figure 2: 3D model (top), top view (middle), and cross section (bottom) of humidity sensor.

The polyimide layer will expand when it absorbs water from the air, which affects the bending of the cantilever and results in the change of resistance of the Pt resistor [5]. By finding the relationship between the RH and the resistance of the Pt resistor, we can know the relative humidity by measuring the resistance.

Airflow Sensor

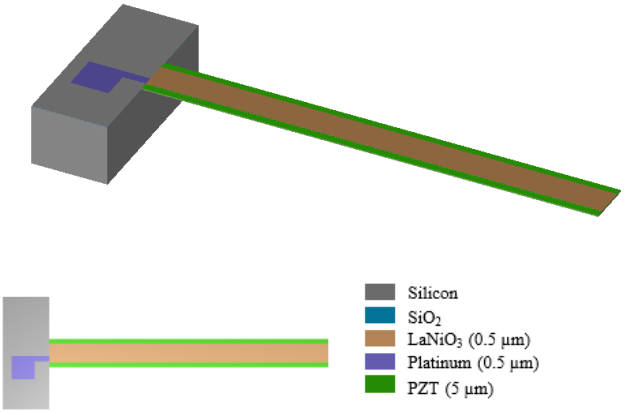

Figure 3: 3D model (top), top view (bottom) of humidity sensor.

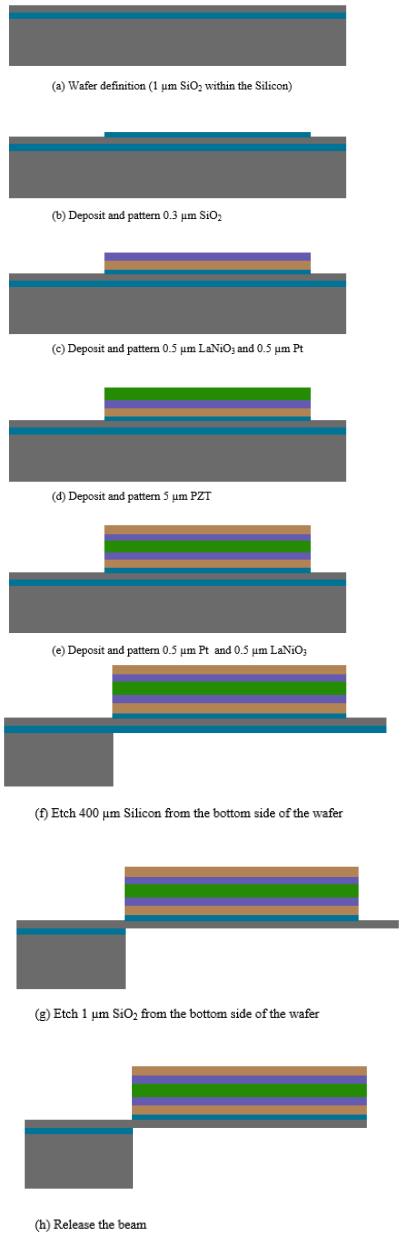

Figure 4: Fabrication process of airflow sensor.

For a cantilever under a uniform, distributed transverse load, the relevant boundary conditions are the following:

$$dy/dx = 0 \text{ at } x = 0 \quad (5)$$
$$y = 0 \text{ at } x = 0 \quad (6)$$

The moment as a function of x can be calculated as the following:

$$M(x) = Fr = [(L - x)f][(L - x)/2] = EI(d^2y/dx^2) \quad (7)$$

Integrating once and applying boundary condition Eq. (5):

$$EI(dy/dx) = \{f[L^3 - (L - x)^3]\}/6 \quad (8)$$

Integrating again and applying boundary condition Eq. (6):

$$y(x) = (f/EI)[(L - x)^4/24 + L^3x/6 - L^4/24] \quad (9)$$

The force per unit length applied by airflow is the following:

$$f = \rho v^2 A/L = \rho v^2 w \quad (10)$$

The moment of inertia of a cantilever loaded in a transverse axis along its thickness is the following:

$$I = wh^3/12 \quad (11)$$

Combining these equations, we get a final expression for the displacement at the tip:

$$y\,(x = L) = 3\rho v^2 L^4/(2Eh^3) \quad (12)$$

Where the Young's Modulus of the composite, E, can be found using the following equation:

$$E^{-1} = wL(h_{PZT}E_{PZT}^{-1} + h_{Pt}E_{Pt}^{-1} + h_{LaNiO3}E_{LaNiO3}^{-1} + h_{si}E_{si}^{-1} \quad (13)$$

Thus, for large tip displacements, a large length, small Young's Modulus, and a small thickness are desired. However, since a large PZT element allows for larger output, there is a tradeoff between thickness and output voltage.

RESULTS

Airflow sensor performance and simulation

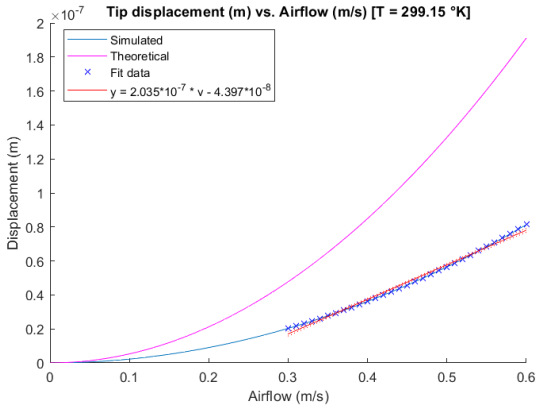

Figure 5: Tip displacement vs. Airflow rate.

$$Tip\ displacement = 2.035*10^{-7}*Airflow - 4.397*10^{-8} \quad (14)$$

R^2 is .992 in the range from .3 to .5 m/s, which indicates that the linear model is a good fit in that range.

Temperature and humidity effects

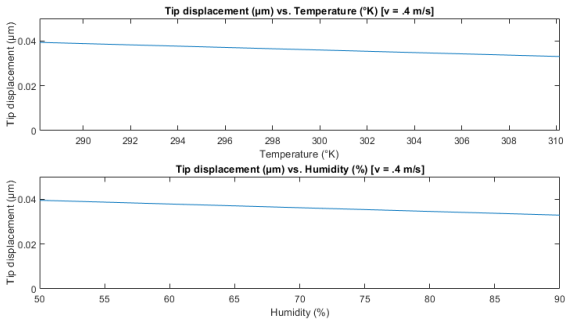

Figure 6: Tip displacement vs. Temperature (top), and Tio displacement vs. Humidity (bottom).

Final design

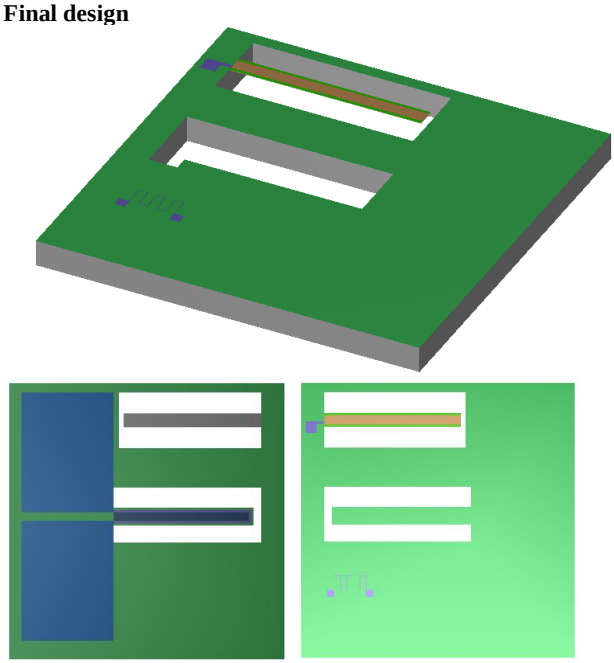

Figure 7: 3D model (top), bottom view (bottom left), and top view (bottom right) of the final design.

DISCUSSION

Effect of humidity and airflow rate on temperature sensor

L.-T. et al. [5] measured the stability of their embedded RTD-type thermal resistor when it is affected by different humidity conditions. According to their measurements, when the humidity range is from 40%RH to 90%RH, the variation in the measured temperature is negligible. In other words, the thermal resistor is isolated from the humidity effects in the range we want the sensor to measure, which is 50%RH to 90%RH.

Since the resistivity and the temperature coefficient resistance (TCR) of the Pt resistor will not be affected by the small airflow rate from .3-.5 m/s, the thermal resistor should be isolated from the airflow rate effects.

Effect of temperature and airflow rate on humidity sensor

Since the sensing mechanism of the humidity sensor is based on the measured resistance of the Pt resistor which is affected by the bending situation of the cantilever, this humidity sensor will be influenced by temperature because it is proven that the tip displacement of the sensor cantilever is dependent on the ambient temperature [5]. With a fixed RH value, the sensitivity (represented by S, unit: KΩ/%RH) increases along with decreasing temperature [5]. L.-T. et al. [5] derived a formula for the relationship between the temperature (represented by T, unit: K) and the sensitivity based on the experimental data:

$$S = 0.0003T^2 - 0.0554T + 3.5305 \quad (15)$$

By combining this equation with Eq.(4), we are able to derive the following equation:

$$\Delta RH = \Delta R/(0.006655R^2 - 0.4017R + 7.035) \quad (16)$$

Therefore, by plugging the resistance of the temperature sensor to the Eq. (16), we can know the change of relative humidity by measuring the change of the resistance of the humidity sensor.

Since the humidity sensor also experiences the force from air, it is reasonable to expect cross-coupling. However, as L.-T. et al. [5] find, the displacements induced by the change in RH are much greater than even the maximum displacement induced by airflow (~.08 μm). Therefore, we expect the effect of airflow to be negligible on the humidity sensor measurement.

Airflow sensor matrix and cross-coupling

Our predicted model of the tip displacement versus airflow overestimated the COMSOL simulated tip displacement by a constant multiplicative factor of 2.35. However, since the simulated result can be obtained from the theoretical result by a constant multiplicative factor, the overall relationship—quadratic with respect to airflow—is correct. Since the factor is less than an order of magnitude, one possible explanation is that it is a result of the specific geometry of the problem that our theoretical model does not account for. Following this result, we ran another simulation with a 10x thicker beam and saw much better agreement between theory and simulation (< 20% error). This supports our hypothesis of a geometric factor correlated to how thin the beam is. The thinner the beam, the less uniform the stress, resulting in deviation from theory. The sensitivity we measured for airflow sensor in the optimal airflow range from .3-.5 m/s was .2 μm/(m/s). Although not ideal, these tip displacements and sensitivities are usable and generate a non-zero voltage output from the piezoelectric. In future work, we hope to increase this sensitivity and reach a cantilever design that experiences greater tip displacement. Furthermore, we hope to elucidate the relationship between tip displacement and output voltage for our MEMS device.

In Figure 6, we see that the effects of humidity and temperature on the tip displacement are very similar. These effects can be explained as follows. By Eq. (10), the force applied by air on the beam is directly related to the density of the air. For a fixed temperature, the density of air decreases linearly with increasing relative humidity, causing a decrease in force, and ultimately reducing the tip displacement. This explains the linear relationship we see between tip displacement and relative humidity. For a fixed humidity, the effect of temperature is slightly more complicated. At higher temperatures, air can hold more water and so becomes less dense since dry air is denser than wet air. At the same time, for a fixed pressure, an increase in temperature will cause an increase in volume which tends to decrease the density. For the range of temperatures we tested, this effect was linear. For both humidity and temperature, the difference between the tip displacement at the lowest and highest values of each range was about 7 nm. By using our model, a difference of 7 nm corresponds to a difference in measured airflow of .034 (m/s). Assuming the difference is similar in the range from .3-.5 m/s, then a rough estimate of the accuracy of our sensor is +/- .034 (m/s). This value offers feasible granularity in the range from .3-.5 (m/s).

Future work

In our fabrication of the integrated sensor, we found that there was significant left-over die area. This presents on opportunity for future work. As earlier cited, another important parameter for vertical farming is the CO_2 level. In the future, it may be possible to utilize the left-over die area to integrate a MEMS CO_2 sensor as well. This would not only allow for more granular sensing for vertical farming, but also reduce cost and waste by eliminating the need for off-chip CO_2 sensors and making maximal use of available die area. Our vision for this work is a vertical farming system in which the environmental factors of every fruit, vegetable, and otherwise can be monitored individually, cheaply, and accurately. Furthermore, a multi-variable model that considers the tip displacement as a function of temperature, humidity, and airflow simultaneously would increase the accuracy of the sensor. A final model relating the tip displacement to voltage output would allow our sensor to be incorporated into wider electrical circuits.

Cost analysis

The cantilevers and thin-film RTD sensor are common structures with established process flows. Because we were able to integrate these three sensors without developing a new or complex process flow, our MEMS sensor can be mass manufactured cheaply. However, the total die area is high which increases the cost. To offset this, integrating more sensors on the unused area as discussed earlier or further optimizing the cantilever dimensions to reduce size are possibilities to explore in future work.

CONCLUSION

In conclusion, we have performed fabrication, design, analysis, and simulation for an integrated MEMS airflow, temperature, & humidity sensor. For the airflow sensor, we were able to fit a linear model to the range from .3-.5 m/s with R^2 = .992. We achieved a sensitivity of .2μm / (m/s) and a rough accuracy of +/- .034 (m/s). These results show promise for the feasibility of a real-world implementation of our design. In future work, we hope to incorporate a CO_2 sensor to reduce the die area wasted; develop a multi-variable model for the airflow sensor that more accurately accounts for the coupling effects of temperature and humidity; and develop a piezoelectric model to elucidate the relationship between the tip displacement and output voltage. Ultimately, with our work as the foundation, we envision MEMS-enabled vertical farming systems capable of precise monitoring and control of individual plants, vegetables, and otherwise.

REFERENCES

[1] Avgoustaki, D. D., & Xydis, G. (2020). How energy innovation in indoor vertical farming can improve food security, sustainability, and food safety? 1–51.

[2] Benyamin Naranjani, Zabihollah Najafianashrafi, Christopher Pascual, Ireneo Agulto, Po-Ya Abel Chuang. Computational analysis of the environment in an indoor vertical farming system, International Journal of Heat and Mass Transfer, Volume 186, 2022, 122460, ISSN 0017-9310.

[3] Rabbi, Barkat & Chen, Zhong-Hua & Sethuvenkatraman, Subbu. (2019). Protected Cropping in Warm Climates: A Review of Humidity Control and Cooling Methods. Energies. 12. 2737. 10.3390/en12142737.

[4] Hatfield, J.L., Boote, K.J., Kimball, B.A., Ziska, L.H., Izaurralde, R.C., Ort, D., Thomson, A.M. & Wolfe, D. (2011), Climate Impacts on Agriculture: Implications for Crop Production. Agron. J., 103: 351-370.

[5] Chen, L.-T., Lee, C.-Y., & Cheng, W.-H. (2008, July 10). MEMS-based humidity sensor with integrated temperature compensation mechanism. Sensors and Actuators A: Physical, Volume 147, Issue 2, 2008, 522-528.

[6] Liu, Huicong, Song, Zhang, Kathiresan, Ramprakash, Kobayashi, Takeshi, & Lee, Chengkuo. Development of piezoelectric microcantilever flow sensor with wind-driven energy harvesting capability, Appl. Phys. Lett. 100, 223905 (2012).